JACS
JOURNAL OF THE AMERICAN CHEMICAL SOCIETY

ARTICLE

pubs.acs.org/JACS

Mechanism for Singlet Fission in Pentacene and Tetracene: From Single Exciton to Two Triplets

Paul M. Zimmerman,*[,†] Franziska Bell,[†,‡] David Casanova,[§] and Martin Head-Gordon*[,†,‡]

[†]Department of Chemistry, University of California, Berkeley, California 94720, United States

[‡]Lawrence Berkeley National Laboratory, Berkeley, California 94720, United States

[§]Institut de Química Teòrica i Computacional, Universitat de Barcelona, Martí i Franquès 1-11, 08028 Barcelona, Spain

Supporting Information

ABSTRACT: Singlet fission (SF) could dramatically increase the efficiency of organic solar cells by producing two triplet excitons from each absorbed photon. While this process has been known for decades, most descriptions have assumed the necessity of a charge-transfer intermediate. This *ab initio* study characterizes the low-lying excited states in acene molecular crystals in order to describe how SF occurs in a realistic crystal environment. Intermolecular interactions are shown to localize the initially delocalized bright state onto a pair of monomers. From this localized state, nonadiabatic coupling mediated by intermolecular motion between the optically allowed exciton and a dark multi-exciton state facilitates SF without the need for a nearby low-lying charge-transfer intermediate. An estimate of the crossing rate shows that this direct quantum mechanical process occurs in well under 1 ps in pentacene. In tetracene, the dark multi-exciton state is uphill from the lowest singlet excited state, resulting in a dynamic interplay between SF and triplet−triplet annihilation.

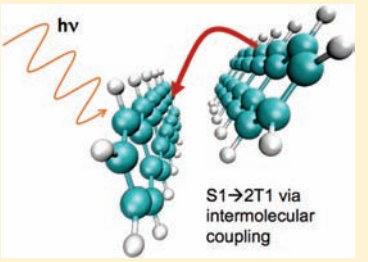

INTRODUCTION

A serious limitation to the efficiency of solar cells is the inability of typical photovoltaic materials to convert a large portion of the solar spectrum into usable energy. Most materials thermalize excess energy above the band gap, which limits the efficiency of solar cells to a maximum of 33%.[1] This limitation, however, can be overcome in materials that convert high-energy photons into multiple electron−hole pairs.[2] In organic semiconductors, this process is known as singlet fission (SF),[3] where the singlet excited state converts into two triplet electron−hole pairs. Besides the efficiency advantage from generating multiple charge carriers from single photons, SF has the advantage of creating long-lived triplet excitons. This makes charge separation—a key issue that must be addressed in organic solar cells—much easier due to the long diffusion lengths of the triplet carriers.

SF has been observed in acene crystals[4−16] and has been suggested to occur in rubrene crystals.[16,17] The process is energetically uphill in tetracene because the energy of two triplets (2T1) exceeds that of the lowest singlet (S1) excited state (i.e., $2E(T1) > E(S1)$).[4−10] Due to this energetic ordering, the reverse process, triplet−triplet annihilation to a single singlet exciton, is also possible. In pentacene, SF is a spontaneous process,[10−16] in part because S1 is greater in energy than 2T1, and therefore little to no triplet−triplet annihilation occurs. Although the energetics must be favorable ($E(S1) \approx 2E(T1)$) for fission to occur, the rate of transition between the optically allowed excited state and the dark multi-exciton (ME) state must also be fast. While the electronic coupling criterion remains little understood, minimal stimulated emission in pentacene[16] suggests that S1 converts into an optically dark state on a rapid time scale. Structurally, tetracene and pentacene crystals take on a similar herringbone configuration (Figure 1) and are neighboring members of the linear acene series, which consists of fused benzene rings. The similarities in geometric and electronic structure between tetracene and pentacene crystals point to the possibility that a unifying mechanism can be found to explain their photoresponse.

In addition to recent experimental studies,[5,11,13−16,19] molecular simulations have been directed at understanding pentacene's photophysics. Specifically, Marciniak et al.[14,15] suggested that excimers (an excited-state dimer complex with locally distorted geometry) form in the pentacene lattice upon photoexcitation to S1, which would account for rapid photobleaching of the S0 → S1 transition. Kuhlman et al.[19] suggested the formation of a bound doubly excited dimer state might account for the long-lived photoinduced absorption. However, these simulations could not capture ME (or doubly excited) states[20] due to limitations in the simulation method (time-dependent density functional theory, TD-DFT[21]). Therefore, most studies up to this point could only model single-exciton states such as S1 and T1, but could make no quantitative predictions for ME states. These limitations have prevented the full verification of any detailed mechanism for SF.

Received: September 6, 2011
Published: November 15, 2011

In addition, there is an ongoing discussion about whether charge-transfer (CT) states are involved in SF.[3,15,19,22] The originally proposed mechanism for SF is based on model Hamiltonians that couple of monomer states between adjacent molecules.[22,23] The low coupling in the model between the single-exciton and ME states requires that a CT state be invoked as an intermediate (i.e., an indirect mechanism). This requires the assumption that the CT state is relatively low in energy and thus energetically accessible. Herein, systematic *ab initio* study of the low-lying excited states in tetracene and pentacene provides an alternative mechanism for the photophysics of these materials. This study provides evidence that CT states need not be directly relevant to SF in acenes. Furthermore, the proposed *direct* mechanism accounts for the nonadiabatic coupling that explains the rapid rate of SF in the acenes.

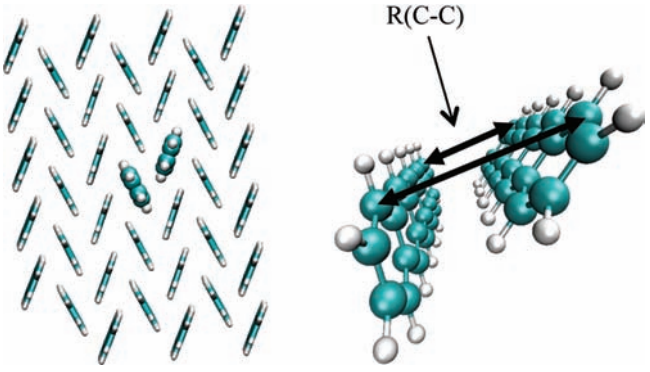

Figure 1. Model herringbone structure of pentacene with active dimer highlighted (left side), which represents one layer of the organic crystal. The π interactions between molecules in the remaining layers (not shown) are much weaker. Active dimer is shown with constraint coordinate R(C−C), which is the distance between the outermost carbon atoms on one side of each pentacene monomer (right side). Decreasing distance along this coordinate results in increased coupling between the two monomers. The structures for tetracene are qualitatively similar to those for pentacene.

This article is arranged as follows. First, a brief description of our *ab initio* simulation methods is provided, including how these can provide a novel description of SF without the use of model Hamiltonians.[24] Second, simulation of the character and spatial extent of low-lying optically bright single-exciton states in pentacene shows that these do not have CT character and can localize to a dimer by geometric relaxation after photoexcitation. Next, simulations of the potential energy surface (PES) of the bright (single-exciton) and dark (double-exciton) states in acene crystals provide a new mechanism for SF proceeding through intermolecular coupling. This mechanism (Scheme 1) both describes the required electronic coupling and accounts for the energetic requirements. An estimate of the transition rate for pentacene is given via Landau−Zener−Stueckelberg theory. Finally, a discussion of the mechanism and some conclusions are provided.

QUANTUM MECHANICAL SIMULATION

To examine tetracene and pentacene photoexcited processes, we employ *ab initio* simulations that describe single-exciton and ME states. These simulations are based on the restricted active space double spin-flip (RAS-2SF) method,[25] which produces a balanced treatment of excited states, including ME states, with a low computational cost (see the Computational Details section for further information). In addition, TD-DFT simulations provide information on the character and delocalization of optically allowed excited states in the acene crystals. While TD-DFT cannot describe ME states, it can efficiently describe the nature of single-exciton states in relatively large clusters of acene monomers.

The geometries of the interacting molecules in the crystal phase are obtained via molecular mechanics (MM) simulations to represent a realistic environment. In order to describe the molecular motion that couples single-exciton to ME states, geometries are optimized with a varying intermolecular coordinate denoted R(C−C). Motion along this coordinate represents increased coupling via increased π orbital overlap of two monomers (see Figures 1 and 2). As shown below, motion along

Scheme 1. Proposed SF Mechanism for Pentacene (Left) and Tetracene (Right)[a]

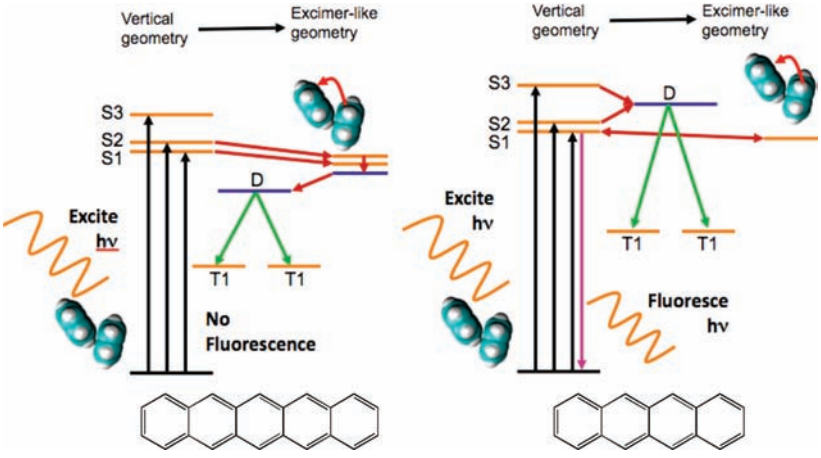

[a] Each of these diagrams can be read as follows. Initial photon absorption occurs at the left-hand side to access the optically bright single-exciton states, S1−S3. Subsequent geometric relaxation can localize such states to an excited-state dimer unit (right side), which can lead to a nonadiabatic transition to the ME state, D (middle). The dark state D directly connects to a pair of triplet states, T1. In each acene, SF occurs when the dimer reaches the dark D state, which is the wave function for two triplets coupled overall to a singlet. Excited-state dimer species can form in either acene, although these states only appear to accelerate SF in pentacene.

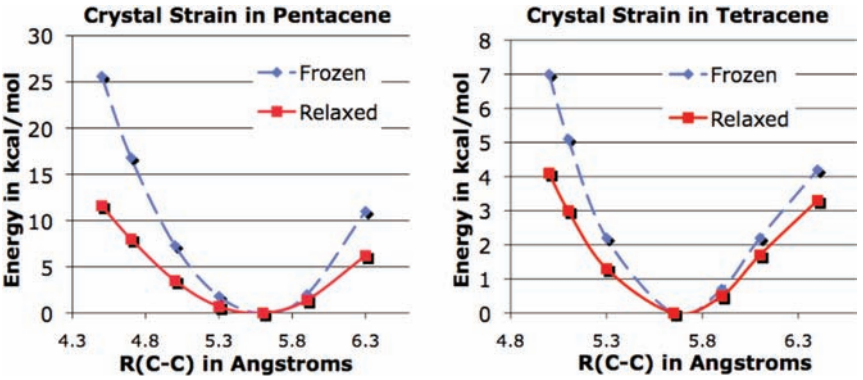

Figure 2. Comparison of crystal response to motion along R(C−C) computed by the MM3 potential for pentacene (left), allowing nearest neighbors to relax vs frozen nearest neighbors. Similar for tetracene (right).

Table 1. Excitation Energies and Dipole Moments from TD-DFT[a]

	pentacene			tetracene		
	energy (eV)	oscillator str.	dipole (D)	energy (eV)	oscillator str.	dipole (D)
			Tetramer			
ground	0.00		1.08	0.00		0.92
S1	2.26	0.378	1.63	2.99	0.435	1.75
S2	2.35	0.080	1.57	3.04	0.160	0.86
S3	2.40	0.034	0.89	3.10	0.112	1.60
S4	2.40	0.109	1.30	3.12	0.010	1.54
S5 (CT)	2.54	0.033	10.75	3.25	0.023	14.77
S6 (CT)	2.62	0.001	9.30	3.34	0.009	14.40
S7 (CT)	2.67	0.015	11.06	3.37	0.007	5.40
S8 (CT)	2.74	0.029	8.54	3.43	0.032	4.34
			Decamer			
ground	0.00		0.80	0		0.930
S1	2.13	0.707	1.16	2.88	0.786	0.859

[a] Due to the large size of the cluster, only the first excitation is available for the 10-monomer cluster.

R(C−C) represents the spontaneous motion of S1 following photoexcitation and is the key coordinate that contributes to SF.

In general, optically allowed excited states are single-exciton states that become populated by photoabsorption that promotes one electron from an occupied orbital to an unoccupied orbital. These states are labeled herein as S*n*, which denote spin singlet single-exciton states. The wave functions are not necessarily localized on monomers but can be delocalized across several closely connected molecules. In contrast to S*n* states, direct absorption of a single photon to a ME state is effectively forbidden and therefore occurs at very low probabilities (two electrons are promoted, giving states that cannot couple to the ground state via the one-electron dipole operator). Therefore, the ME states are labeled D because they are optically dark. Examination of the wave function character from RAS-2SF reveals that D represents two triplet excitons coupled overall to a singlet in the dimer pair. The method correctly represents D by predicting the energy of the dark state, E(D), to be exactly equal to the energy of two triplets in a simulation of two isolated monomers.

Because these *ab initio* simulations capture the correlation of many electrons, they are distinct from model Hamiltonian studies (for instance ref 22). The current understanding of SF comes from model Hamiltonians, where certain electronic states of two monomers are employed as basis sets. While model Hamiltonian studies can yield deep insights into complex physical processes such as SF, these invariably require assumptions about the physics which are embedded as model parameters. By contrast, *ab initio* calculations in principle allow the essential features to emerge directly from simulations. This means that RAS and TD-DFT simulations automatically determine the extent of CT character in each state, as well as the extent of exciton delocalization. These methods are computationally fast enough to simulate multiple geometric configurations in acene dimers, allowing for description of the effect of molecular motion on quantum mechanical coupling between states. In particular, RAS can capture both singly and multiply excited states such as the S*n* and D excitations that are energetically low-lying and most relevant to SF.

■ CHARACTER AND LOCALIZATION OF OPTICALLY ALLOWED EXCITONS IN PENTACENE

Before examining how the bright single excitations can transition to dark ME states, the nature of single excitons in acene

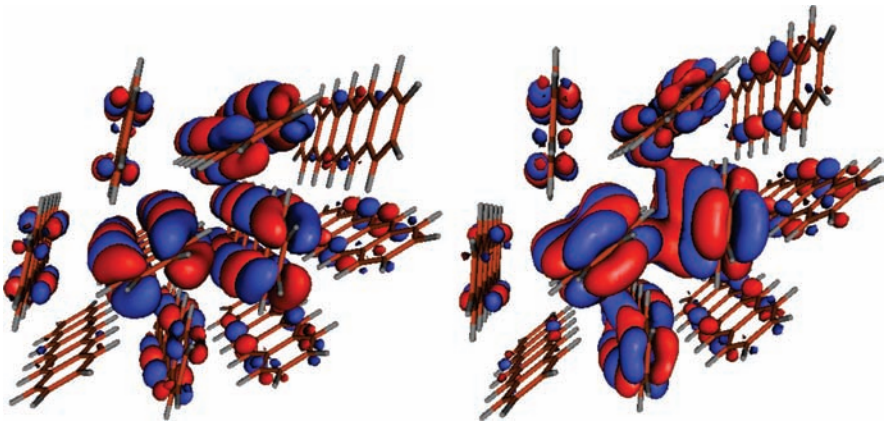

Figure 3. Natural transition orbitals for the S1 vertical exciton in pentacene: left, electron; right, hole. The spatial overlap between electron and hole shows that this is not a charge transfer exciton, but a nonpolar electron−hole pair delocalized over four monomers.

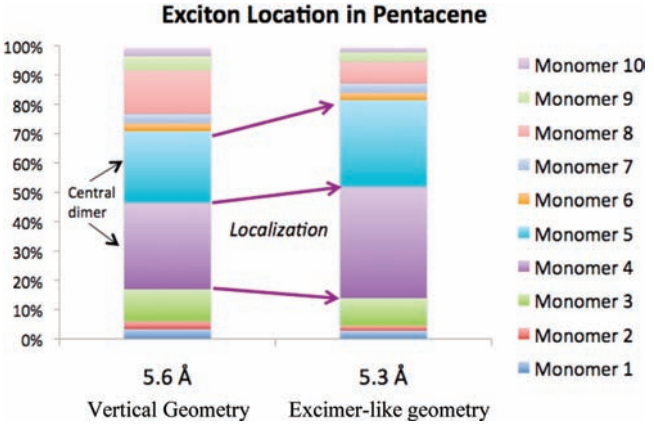

Figure 4. Extent of localization of the S1 excitation in pentacene at the vertical (R(C−C) of 5.6 Å, as defined in Figure 1) and excimer-like (R(C−C) relaxed to 5.3 Å) structures. Monomers 4 and 5 correspond to the central monomers in the acene cluster, and it is evident that the vertical excitation increases from 56% localized on this pair to 71% at the relaxed excimer-like geometry. The percentage of the exciton on each monomer is obtained through NTO analysis.[26]

crystals will be described. Due to the cost of TD-DFT, simulations of a cluster of 10 pentacene monomers are possible, but this is at the upper limit of computational feasibility. It is found below that 10 monomers are sufficient to quantify the delocalization of the S1 exciton. A more computational tractable simulation involving four monomers (the four most important monomers of the fully delocalized wave functions, *vide infra*) is also performed to analyze a range of excited states. While these simulations only capture single-exciton states, any amount of CT character in these states will naturally be included.

Table 1 lists the TD-DFT excitation energies, oscillator strengths, and dipole moments for the excited states of the two acenes. The oscillator strengths indicate that the first few Sn excitations are the bright states that will be populated via photoexcitation. The TD-DFT dipole moments from the four pentacene cluster indicate that the lowest energy Sn excitations in pentacene and tetracene have no CT character. The higher excited states (S5 and on) do have CT character, but these states have low oscillator strengths and are significantly above the lowest energy states. In order for CT states to contribute to the SF process, additional energy is required.

Figure 3 shows the most important natural transition orbitals (NTOs)[26] for pentacene S1 in a decamer cluster. These orbitals represent the electron−hole pair of the excited state (this configuration represents 81% of the state) and are useful for determining wave function character and spatial extent of the exciton. Most of the S1 exciton is localized on the two central monomers, with significant contributions from two neighboring monomers. Therefore, the wave function is delocalized over approximately four monomers, with another four monomers contributing in smaller amounts. The spatial overlap between electron and hole contributions is large, verifying the dipole moment analysis that shows S1 is not a CT exciton. This analysis contrasts with a recent study[27] that suggested significant amounts (∼50%) of CT character in the lowest excited states of acene crystals. The study described the excitations using a model Hamiltonian which was parametrized on the basis of monomer excitation data. The present first-principles study, which required no assumptions about the character of the excited states, suggests mixing of CT character into the lowest-lying bright states does not in fact occur. This conclusion should be robust with respect to improvements in the density functionals used in TD-DFT because the current functional tends to underestimate CT excitation energies.[21]

Additional analysis on the location of the electron hole pairs can be performed to give exciton contributions that are specific to each monomer. This is shown in Figure 4, which quantifies the amount of electron−hole pair per monomer. Interestingly, decreasing the distance between the two central molecules via reducing the R(C−C) distance (defined in Figure 1) localizes the wave function even further. This motion corresponds to a formation of an excited-state dimer (which will be described further in the next section). The dipole moment for this species, 0.72 D, is similar to that of the ground state, which indicates that the state does not develop CT character upon this geometric shift. TD-DFT predicts that the motion along R(C−C) from 5.6 Å to 5.3 Å is exothermic, indicating that immediately after photoexcitation the exciton will localize spontaneously by relaxation to an excimer-like configuration.

■ COUPLING OF SINGLE- AND MULTIPLE-EXCITON STATES VIA INTERMOLECULAR MOTION

Because the bright excited states have been shown to localize to a dimer with decreasing monomer−monomer distance, the

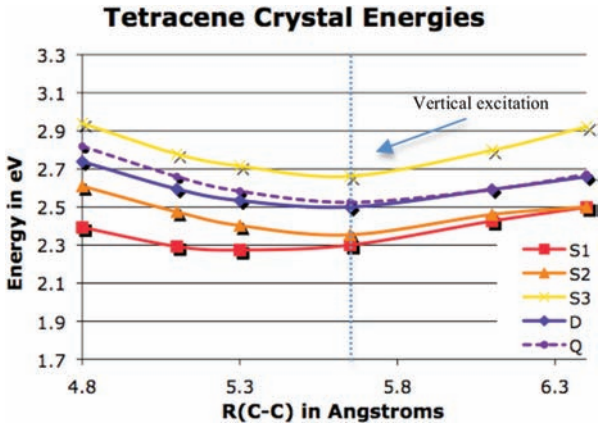

Figure 5. RAS potential energy surfaces along the R(C−C) coordinate for tetracene, including the lowest four singlet excited states (single-exciton S1−S3 and multi-exciton D) and the quintet (Q). The vertical excitation occurs at the ground-state geometry, where R(C−C) = 5.65 Å.

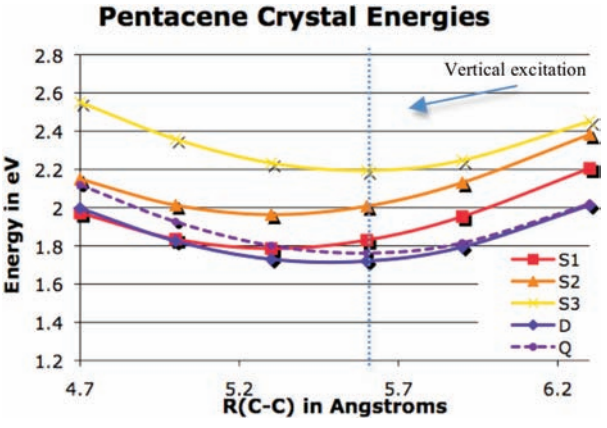

Figure 6. RAS potential energy surfaces along the R(C−C) coordinate for pentacene, including the lowest four singlet excited states (single-exciton S1−S3 and multi-exciton D) and the quintet (Q). The vertical excitation proceeds at the ground-state geometry, where R(C−C) = 5.6 Å.

mechanism for SF can potentially be described via RAS simulations of the low-lying excited states of the dimer embedded in the crystal environment. The PESs shown in Figures 5 and 6 show RAS results that predict how excited-state dimers interact with the ME state D in acene crystals. Excited-state dimers of S1 are slightly favored relative to the vertical geometry by approximately 0.03−0.04 eV in both acene crystals. These excimer-like structures exist along the R(C−C) (see Figure 1) coordinate about 0.3 Å shorter than the ground-state minimum, which is not a large shift in monomer positions. Two previous studies of pentacene sandwich complexes[15,20] suggested that a face-to-face excited-state dimer could be favorable by up to ∼0.3 eV compared to distantly separated monomers. These results with isolated monomers neglected the acene herringbone structure in addition to the lattice strain, so 0.3 eV represents an upper limit to this value. In a more realistic environment, a parallel face-to-face configuration is not possible due to the lattice strain. The energy cost for forming a face-to-face dimer at an R(C−C) value of 4.0 Å is approximately 1.6 eV, which is far above the maximum stabilization energy of 0.3 eV which could be recovered. In addition to the S1 excited-state dimer, an excited-state dimer of S2 appears to be possible in pentacene, but not in tetracene. Therefore, although the excimer-like species are weakly bound and result from only small structural changes in the acene lattice, they do represent a real local minimum on the excited-state surface, distinct from the ground-state geometry.

To better understand the excited-state interactions, the components of the total energy are separated into excited-state and lattice strain energies in Table 2. In pentacene, RAS-(4,4)-2SF predicts S1 and S2 drop in energy by ∼0.09 eV from the 5.6 Å to the 5.3 Å dimer geometry (TD-DFT predicts S1 drops 0.10 eV and S2 drops 0.03 eV). This energy must be compared to the lattice strain of ∼0.04 eV. Overall, this creates a net stabilization of the excimer-like structure relative to the vertical geometry. In comparison, the ground state goes up in energy 0.01 eV over the same distance, indicating that these geometric changes encounter a relatively soft resistance from the crystal lattice. In tetracene, the dimer component of binding in S1 is 0.09 eV and in S2 is 0.01 eV. Therefore, when lattice strain is included, the S1 excited-state dimer is favorable but the S2 excited-state dimer is not. Because excited-state dimers are favorable, photoexcited states in tetracene (S1) and pentacene (S1, S2) will quickly shift into these configurations. This will occur on the time frame of the R(C−C) vibrational period, which we estimate from simulations to be around 250 fs in each acene.

Figures 5 and 6 suggest how the excited electronic states may couple to undergo SF. If any of the Sn states populated by the initial photon absorption become close to degenerate with D at accessible geometric configurations, nonadiabatic transitions rapidly transfer population between the two states.[38−41] If D is lower in energy than Sn, the overall population transfer will be downhill from Sn to the D state. Otherwise, if D is higher in energy than Sn, additional energy, for example from lattice vibrations, will be required to populate the D state. In either case, the nonadiabatic transition arises from the close proximity of the states, but uphill population transfer to D still comes with an energetic cost. Therefore in pentacene, the PES in Figure 6 suggests that the population transfer will proceed directly and rapidly downhill following photoexcitation. In tetracene, however, Figure 5 predicts there is an small uphill energy gap that slows total population transfer of S1 into D due to the need for additional energy.

The rate of population transfer between excited states can be qualitatively described by considering the nonadiabatic coupling between the states and the nuclear velocities. When adiabatic states become degenerate, the Born−Oppenheimer approximation breaks down because the wave function cannot be described by a single adiabatic state. In this limit, nuclear motion along with strong nonadiabatic coupling (proportional to $1/\Delta E$) causes rapid population transfer between the states. When two states are well separated in energy, there is little coupling between states and each is likely to stay on the adiabatic surface. In this case, large nuclear velocities are required to couple nuclear and electronic motion and thus transition between adiabatic surfaces. In acenes, the adiabatic states are relatively close in energy, but do not reach exact degeneracies along the R(C−C) coordinate. This near degeneracy, combined with significant R(C−C) velocity, is an intermediate situation where the adiabatic approximation partly breaks down, and significant population transfer can take place.

To quantify the rate of population of D from S1 in pentacene, the most reliable method is to compute the nonadiabatic

Table 2. Dimer, Crystal, and Total Energies (in eV) for Tetracene and Pentacene at the Vertical (Vert.) and Excited-State Dimer (Exc.) Geometries from RAS-(4,4)-2SF/MM3[a]

	total energy (dimer energy) (ev)					
	S0	S1	S2	S3	D	crystal strain
			Tetracene			
Vert.	0.00 (0.00)	2.30 (2.30)	2.35 (2.35)	2.66 (2.66)	2.50 (2.50)	0.00
Exc.	0.05 (−0.01)	2.27 (2.21)	2.40 (2.34)	2.72 (2.6)	2.53 (2.47)	0.06
			Pentacene			
Vert.	0.00 (0.00)	1.83 (1.83)	2.01 (2.01)	2.19 (2.19)	1.72 (1.72)	0.00
Exc.	0.01 (−0.03)	1.79 (1.74)	1.96 (1.92)	2.23 (2.19)	1.73 (1.69)	0.04

[a] Exc. and Vert. R(C−C) are 5.3 and 5.65 Å, respectively.

coupling vector. Unfortunately this is not currently available for the RAS-2SF method, so instead Landau−Zener−Stueckelberg (LZS) theory was employed. LZS theory[40−43] allows an estimate of the probability of transition from S1 to D near the crossing region near R(C−C) = 4.9 Å. Standard LZS breaks down at energies near or below the crossing region, but complete equations including tunneling have been derived.[42,43] This theory requires energetic information about the crossing region, including electronic coupling between states and knowledge of the total energy available to reach the crossing region. All of this information can be determined from the current electronic structure computations. A full description of LZS theory is available,[42,43] so the lengthy working equations will not be included in the present article. A detailed description of the LZS calculation is available in the Supporting Information.

In order to perform the LZS calculation, the electronic coupling (denoted H12) between diabatic S1 and D states is required. Because the wave functions from the RAS method are adiabatic, appropriate diabatic states were obtained as described in the Computational Details. The electronic coupling accounts for the degree to which the two diabatic wave functions will mix at near degeneracies, and low values imply near degeneracies between adiabatic wave functions are possible. For example, at the face-to-face sandwich geometry of two monomers, S1 and D have different symmetries and thus H12 becomes exactly zero. Deviations from the face-to-face geometry induce small increases in H12, so small H12 values in the herringbone structure are expected. Furthermore, smaller values of R(C−C) in the herringbone structure are closer to a face-to-face structure, allowing H12 to decrease along the excimer-like coordinate. The computation of H12 between S1 and D shows that H12 is relatively small, 0.00018 au at R(C−C) = 5.6 Å. This small value of H12 allows the two states to become nearly degenerate, so crossing can be very fast. Assuming a vertical excitation from S0→S1, the total energy available is 1.83 eV. With this amount of available energy to reach the crossing region at 1.86 eV (R(C−C) ≈ 4.9 Å), LZS predicts an S1→D transition probability of 16%. Allowing 1 quanta of extra vibrational energy (0.016 eV) increases this probability to 26%. This large probability suggests that a motion along R(C−C) will result in rapid nonadiabatic population of D. The state crossing therefore occurs on the time scale of vibration along R(C−C) (i.e., sub-picosecond time scales).

Having estimated the crossing rate of S1 to D, the fate of the two triplet excitons can be hypothesized. Simulations of the dimer pair at long separation (see Supporting Information) show no binding energy for the two triplets, and therefore the triplets in D are not constrained to remain in the dimer. Because the two triplets can diffuse away from the dimer (the unbound nature of the two triplets is suggested by refs 13 and 16), triplet separation will slow recombination into S1. While it has also been suggested that the two triplets are bound together on neighboring monomers,[19] RAS simulations, which are the first quantum mechanical description of D in the acene crystals, provide no evidence that the triplets are lower in energy when they are in close proximity.

DISCUSSION

To understand how intermolecular motion leads to coupling between Sn and D states, the energetics of the process must first be understood. In tetracene, S1 and S2 are below D in energy (by 0.25 and 0.15 eV), and therefore must undergo thermal activation for significant amounts of crossing into D. This activation energy for SF is near the reported experimental values[3] (0.15−0.24 eV). S3, however, is higher in energy than D, so population of D can proceed downhill from S3. This explains the SF activation barrier and the fraction of excitons that undergo fission without barrier in tetracene (ie S3 excitations),[10,11] because photoabsorption will populate S1−S3, which are in a relatively narrow energy range. The close energetic proximity of Sn and D allows for strong nonadiabatic coupling between the states, but the energy ordering of the states will still control the overall populations of D relative to Sn.

In pentacene, S1−S3 have energies higher than D, making SF exothermic. As pentacene's S1 state relaxes to the excited-state dimer due to its slight energetic favorability (∼0.04 eV), D increases in energy, becoming within 0.06 eV of S1 at the excited-state dimer geometry. S1 and D become nearly degenerate at a separation of 5.0 Å, where the crossing can be described as narrowly avoided[45] due to weak electronic coupling between the states (in the D_{2h} sandwich geometry, S1 is B_{1g} and D is A_g[20] and the electronic coupling is exactly zero). The weak electronic coupling ensures the states can closely approach one another, allowing fast nonadiabatic transition. LZS theory shows that the probability of transfer from S1 to D is around 20%, indicating that transition will be efficient in the region around the excited-state dimer.[38−43] Therefore in pentacene, transition from S1 to D occurs on the time scale of intermolecular motion along R(C−C) (sub-picosecond time scales).

Although nonadiabatic transition in pentacene is expected to be fast and complete due to the near degeneracy and exothermicity, for tetracene, D is uphill from S1 and S2. Instead, S2 and D might become nearly degenerate by vibrational excitation, leading to SF. This can occur by thermal fluctuations, suggesting that

the activation energy for SF in tetracene can be explained by excitation of specific intermolecular coupling modes. By analogous analysis of the reverse process, triplet−triplet annihilation in tetracene is energetically downhill by D converting into S1 or S2, but is a thermally activated process in pentacene because S*n* states are all higher in energy than D. This is in agreement with experiment, which shows little fluorescence from pentacene and delayed fluorescence in tetracene.

Because SF from S1 is energetically uphill, it might be controlled by selective excitation of vibrational modes during photoexcitation to S1 or S2. Recently, enhanced SF in tetracene was observed by pulse-shaping experiments.[44] These experiments suggested that selective excitation of intermolecular vibrations could increase triplet yield. This situation could be interpreted as increased intermolecular coupling caused by excitation of vibrational modes that are qualitatively similar to motion along *R*(C−C). This excitation provides increased motion along the intermolecular coordinate as well as increased energy to shift S1 population into D.

From the results presented herein, the mechanism for SF can be represented by Scheme 1. Because intersystem crossing to monotriplet states is slow compared to SF time scales ($\tau_{SF} \ll 1\ \mu s$[5,10,11,14]), higher spin states than singlets are not considered. This mechanism is in accordance with recent experimental findings,[5,10,11,13−16] including photobleaching of the S0→S1 transition that occurs on a 80 fs time scale in pentacene.[14,15] Contrary to previously suggested mechanisms, the proposed mechanism does not involve CT intermediates. These CT intermediates are not necessary for SF because direct coupling of S*n* to D is possible. Furthermore, TD-DFT simulations indeed show the lowest energy excited states do not contain significant CT character.

Because D is not a bound state, the two triplets of D can diffuse away from the initial dimer without significant barrier. The triplets produced by the SF process can be spectroscopically identified by their long lifetime and energetic location of absorption peak. In a tetracene (pentacene) dimer, TD-DFT computes the T1 → T2 absorption to occur at 1.53 eV (1.33 eV). These peaks match the location of the long-lived absorption peaks from experiment,[10,11] suggesting that triplets can be identified by pump−probe spectroscopy.

CONCLUSIONS

This study provides two important contributions to understanding singlet fission in acene crystals: (1) localization of S*n* states via formation of an excimer-like state (from TD-DFT), and (2) coupling along the same intermolecular coordinate that leads to rapid population of the D state (from RAS and LZS). In acene crystals, localization of the S1 exciton through intermolecular motion facilitates state crossing to a localized triplet−triplet ME state on a dimer. This allows a description of the acene photoresponse from coupling between a pair of acene monomers.

The behavior of the S*n* and D states in the acene crystals dictate their photoresponses and also provide an explanation of how acene molecules couple during SF. Increasing the π overlap between neighboring monomers via excited-state dimer formation increases the energy of D while the energy of S1 decreases. This coupling provides a natural avenue for state transition in pentacene by creating a near-degeneracy between S1 and D. In tetracene, the downhill non-adiabatic transition from S3 into D does not appear to occur through excited-state dimers, but likely proceeds through another relaxation coordinate. The specific coordinate responsible for unactivated SF in tetracene will require additional investigation, while vibrational excitation along the excited-state dimer coordinate can explain the uphill pathway from S1/S2 to D.

This study suggests recently developed *ab initio* methods can explain the complex photoinduced phenomenon in organic semiconductors. These methods describe the intermolecular coupling and ultrafast transition from S1 to D that occur in acene crystals to produce multiple triplet excitons. Furthermore, because RAS-(4,4)-2SF has a relatively low computational cost, it will be applicable beyond SF in acenes. Although TD-DFT descriptions are often useful, more advanced methods must be used to capture ME states that govern the SF process. The molecular level description of acene photophysics described herein provides the key insight of how intermolecular motion leads to SF, and weak coupling between monomers will likely result in slower SF. This insight can serve as a design principle for developing new materials to exploit a maximum portion of the solar spectrum.

COMPUTATIONAL DETAILS

While inexpensive computation tools such as TD-DFT[21] are seeing widespread use, most will not predict the existence of states dominated by two electron excitations, such as ME states. In order to overcome this limitation, while keeping relatively low computational cost, methods such as RAS-2SF and double spin-flip equation of motion coupled cluster have been developed.[24] These methods are based on single-reference wave functions (requiring only one determinant), which avoid the prohibitive computational costs of complete active space self-consistent field (CASSCF) or multi-reference perturbation theory (MRMP) and yield accurate results. This is achieved using a high spin quintet reference, and the excited singlet, triplet and quintet states are obtained simultaneously by double spin-flip excitations ($\alpha \rightarrow \beta$) in the four orbital active space. In the RAS-2SF method utilized in this study, single excitations are permitted from the inactive to the active space and vice versa. The applicability of RAS-2SF was verified by comparison to CASSCF results for the pentacene dimer. Figure S1 of the Supporting Information shows RAS-2SF quantitatively reproduces CASSCF PESs, indicating that RAS-2SF is a suitable replacement for CASSCF in acene dimers.

One deficiency of CASSCF and RAS-2SF theories is the overestimation of excitation energies due to the limited degree of dynamic correlation. To overcome this difficulty, we shift the excitation energies of T1 and S1 at the equilibrium geometry to the experimental values for the acene crystals.[10,11] D is referenced to 2*E*(T1) and S2 and S3 are referenced to S1 (although RAS-(4,4)-2SF does predict *E*(D) within 0.2 eV). This is a uniform shift in the energy that is applied at all geometries to approximate the effect of missing dynamic correlation in the RAS method. Because changes in excitation energy with geometric change are expected to be modeled correctly by CASSCF or RAS-2SF,[28,29] this approximation yields accurate and useful PESs.

In order to estimate the electronic coupling (H12) between S1 and D, diabatic wave functions were generated by applying restrictions to S1 and D wave functions. S1 was restricted to be a singles and triples excited state, while D was restricted to be a purely doubles and quadruples excited state in the four-electron, four-hole orbital active space. This restriction was deemed appropriate because over 90% of each adiabatic wave function could be described by these electronic configurations. Furthermore, in a D_{2h} face-to-face structure, these diabatic states are equivalent to the adiabatic states due to the symmetry constraints, which confirms their suitability.

Model acene crystals[29] contain 37 tetracene or 39 pentacene monomers. These geometries are optimized utilizing the MM3 force field,[31,32] which produces accurate geometries[32] and energies[33] for aromatic hydrocarbons. This force field has been successfully employed in simulations of acene crystal nucleation,[33,34] indicating its suitability for modeling tetracene and pentacene. The outer acene molecules in these structures are frozen (except the hydrogens), leaving an inner acene dimer and its nearest neighbors to relax. Constraints on monomer separation are applied via harmonic potentials. Lattice strain is determined by subtracting isolated dimer energies from the overall system energy. Since RAS-2SF does not describe dispersion, a dispersion correction is applied by shifting all RAS-2SF states such that the energy of the ground state matches the MM3 energy (i.e., $E^{MM3/S0}(r) = E^{QM/S0}(r) + E^{DISP}(r)$).

The results presented herein are dispersion-corrected-RAS-2SF/6-31G* energies that are summed with the lattice strain from MM3. This QM/MM technique includes the energetics of the lattice deformation as well as the excited-state response in the acene dimers. To provide additional confirmation of the RAS-2SF results, we recomputed the dimer energies of the S*n* excited states using TD-DFT and the ωB97X-D functional.[30] When summed with the crystal strain, TD-DFT predicts a slightly larger excited-state dimer binding energy than RAS-2SF, providing further evidence that our excitation energy profiles are meaningful. These same simulations are used along with Natural Transition Orbital[26] analysis to characterize S*n* states in larger acene clusters. All QM computations are performed using a development version of Q-Chem' and MM3 computations are performed using Tinker.[37]

■ ASSOCIATED CONTENT

Supporting Information. RAS-(4,4)-2SF vs CASSCF potential energy surfaces, optimized geometries, and a description of the Landau−Zener−Stueckelberg transition probability calculation. This material is available free of charge via the Internet at http://pubs.acs.org.

■ AUTHOR INFORMATION

Corresponding Author
paulzim@berkeley.edu; mhg@cchem.berkeley.edu

■ ACKNOWLEDGMENT

This work was supported by the Director, Office of Science, Office of Basic Energy Sciences, of the U.S. Department of Energy under Contract No. DE-AC02-05CH11231.

■ REFERENCES

(1) Shockley, W.; Queisser, H. J *J. Appl. Phys.* **1961**, *32*, 510.
(2) Hanna, M. C.; Nozik, A. J. *J. Appl. Phys.* **2006**, *100*, 074510.
(3) Smith, M. B.; Michl, J. *Chem. Rev.* **2010**, *110*, 6891.
(4) Singh, W. J.; Jones, W.; Siebrand, B. P.; Stoicheff; Schneider, W. G. *J. Chem. Phys.* **1965**, *42*, 330.
(5) Burdett, J. J.; Muller, A. M.; Gosztola, D.; Bardeen, C. J *J. Chem. Phys.* **2010**, *133*, 144506.
(6) Groff, R. P.; Avakian, P.; Merrifield, R. E. *Phys. Rev. B* **1970**, *1*, 815.
(7) Geacintov, N.; Pope, M.; Vogel, F. *Phys. Rev. Lett.* **1969**, *22*, 593.
(8) Pope, M.; Swenberg, C. E. *Electronic Processes in Organic Crystals and Polymers*, 2nd ed.; Oxford University Press: New York, 1999.
(9) Burgos, J.; Pope, M.; Swenberg, C. E.; Alfano, R. R. *Phys. Status Solidi* **1977**, *83*, 249.
(10) Thorsmolle, V. K.; Averitt, R. D.; Demsar, J.; Smith, D. L.; Tretiak, S.; Martin, R. L.; Chi, X.; Crone, B. K.; Ramirez, A. P.; Taylor, A. J. *Phys. Rev. Lett.* **2009**, *102*, 017401.
(11) Thorsmolle, V. K.; Averitt, R. D.; Demsar, J.; Smith, D. L.; Tretiak, S.; Martin, R. L.; Chi, X.; Crone, B. K.; Ramirez, A. P.; Taylor, A. J. *Physica B* **2009**, *404*, 3127.
(12) Jundt, C.; Klein, G.; Sipp, B.; Le Moigne, J.; Joucla, M.; Villaeys, A. A. *Chem. Phys. Lett.* **1995**, *241*, 84.
(13) Lee, J.; Jadhav, P.; Baldo, M. A. *Appl. Phys. Lett.* **2009**, *95*, 033301.
(14) Marciniak, H.; Fiebig, M.; Huth, M.; Schiefer, S.; Nickel, B.; Selmaier, F.; Lochbrunner, S. *Phys. Rev. Lett.* **2007**, *99*, 176402.
(15) Marciniak, H.; Pugliesi, I.; Nickel, B.; Lochbrunner, S. *Phys. Rev. B* **2009**, *79*, 235318.
(16) Rao, A.; Wilson, M. W. B.; Hodgkiss, J. M.; Albert-Seifried, S.; Bassler, H.; Friend, R. H. *J. Am. Chem. Soc.* **2010**, *132*, 12798.
(17) Rumyantsev, B. M.; Lesin, V. I.; Frankevich, E. L. *Opt. Spectrosc.* **1975**, *38*, 89–92.
(18) Najafov, H.; Lee, B.; Zhou, Q.; Feldman, L. C.; Podzorov, V. *Nat. Mat.* **2010**, *9*, 938.
(19) Kuhlman, T. S.; Kongsted, J.; Mikkelsen, K. V.; Moller, K. B.; Solling, T. I. *J. Am. Chem. Soc.* **2010**, *132*, 3431.
(20) Zimmerman, P. M.; Zhang, Z.; Musgrave, C. B. *Nat. Chem.* **2010**, *2*, 648.
(21) (a) Runge, E.; Gross, E. K. U. *Phys. Rev. Lett.* **1984**, *52*, 997. (b) Dreuw, A.; Head-Gordon, M. *Chem. Rev.* **2005**, *105*, 4009.
(22) Greyson, E. C.; Vura-Weis, J.; Michl, J.; Ratner, M. A. *J. Phys. Chem. B* **2010**, *114*, 14168–14177.
(23) Jortner, J.; Rice, R. A.; Katz, J. L.; Choi, S.-I. *J. Chem. Phys.* **1965**, *42*, 309.
(24) Psiachos, D.; Mazumdar, S. *Phys. Rev. B* **2009**, *79*, 155106. Guo, F.; Chandross, M.; Mazumdar, S. *Phys. Rev. Lett.* **1995**, *74*, 2086.
(25) (a) Casanova, D.; Slipchenko, L. V.; Krylov, A. I.; Head-Gordon, M. *J. Chem. Phys.* **2009**, *130*, 044103. (b) Casanova, D.; Head-Gordon, M. *Phys. Chem. Chem. Phys.* **2009**, *11*, 9779.
(26) Martin, R. L. *J. Chem. Phys.* **2003**, *118*, 4775.
(27) Yamagata, H.; Norton, J.; Hontz, E.; Olivier, Y.; Beljonne, D.; Bredas, J. L.; Silbey, R. J.; Spano, F. C. *J. Chem. Phys.* **2011**, *134*, 204703.
(28) Rocha-Rinza, T.; De Vico, L.; Veryazov, V.; Roos, B. O. *Chem. Phys. Lett.* **2006**, *426*, 268.
(29) Fink, R. F.; Pfister, J.; Zhao, H. M.; Engels, B. *Chem. Phys.* **2008**, *346*, 275.
(30) Holmes, D.; Kumaraswamy, S.; Matzger, A. J.; Vollhardt, K. P.C *Chem.—Eur.J.* **1999**, *5*, 3399.
(31) Allinger, N. L.; Yuh, Y. H.; Lii, J.-H. *J. Am. Chem. Soc.* **1989**, *111*, 8551.
(32) (a) Lii, J.-H.; Allinger, N. L. *J. Am. Chem. Soc.* **1989**, *111*, 8576. (b) Allinger, N. L.; Li, F.; Yan, L.; Tai, J. C. *J. Comput. Chem.* **1990**, *11*, 868.
(33) Verlaak, S.; Steudel, S.; Heremans, P.; Janssen, D.; Deleuze, M. S. *Phys. Rev. B* **2003**, *68*, 195409.
(34) Goose, J. E.; Clancy, P. *J. Phys. Chem. C* **2007**, *111*, 15653.
(35) Chai, J.-D.; Head-Gordon, M. *Phys. Chem. Chem. Phys.* **2008**, *10*, 6615.
(36) Shao, Y.; et al. *Phys. Chem. Chem. Phys.* **2006**, *8*, 3172.
(37) Ponder, J. W., *TINKER*, Software Tools for Molecular Design; Washington University School of Medicine: Saint Louis, MO, 2001.
(38) Matsika, S. In *Reviews in Computational Chemistry*; Lipkowitz, K. B., Cundari, T. R., Boyd, D. B., Eds.; John Wiley & Sons, Inc.: Hoboken, NJ, 2007; Vol. 23, p 82.
(39) Yarkony, D. R. *Acc. Chem. Res.* **1998**, *31*, 511.
(40) Zener, C. *Proc. R. Soc. London* **1932**, *137*, 696.
(41) Zener, C. *Proc. R. Soc. London* **1933**, *140*, 660.

(42) Nakamura, H.; Zhu, C. *Comments At. Mol. Phys.* **1996**, *32*, 249–266.
(43) Nakamura, H.; Zhu, C. *J. Chem. Phys.* **1995**, *102*, 7448.
(44) Grumstrup, E. M.; Johnson, J. C.; Damrauer, N. H. *Phys. Rev. Lett.* **2010**, *105*, 257403.
(45) Salem, L.; Leforestier, C.; Segal, G.; Wetmore, R. *J. Am. Chem. Soc.* **1975**, *97*, 479.